

Real Time Quarkonium Transport Coefficients in Open Quantum Systems from Euclidean QCD

Bruno Scheihing-Hitschfeld^{1,*} and Xiaojun Yao^{2,†}

¹*Center for Theoretical Physics, Massachusetts Institute of Technology, Cambridge, MA 02139, USA*

²*InQubator for Quantum Simulation, Department of Physics,
University of Washington, Seattle, WA, 98195, USA*

(Dated: June 26, 2023)

Recent open quantum system studies showed that quarkonium time evolution inside the quark-gluon plasma is determined by transport coefficients that are defined in terms of a gauge invariant correlator of two chromoelectric field operators connected by an adjoint Wilson line. We study the Euclidean version of the correlator for quarkonium evolution and discuss the extraction of the transport coefficients from this Euclidean correlator, highlighting its difference from other problems that also require reconstructing a spectral function, such as the calculation of the heavy quark diffusion coefficient. Along the way, we explain why the transport coefficient γ_{adj} differs from γ_{fund} at finite temperature at $\mathcal{O}(g^4)$, in spite of the fact that their corresponding spectral functions differ only by a temperature-independent term at the same order. We then discuss how to evaluate the Euclidean correlator via lattice QCD methods, with a focus on reducing the uncertainty caused by infrared renormalons in determining the renormalization factor nonperturbatively.

I. INTRODUCTION

The scientific mission of relativistic heavy ion colliders is to investigate properties of the deconfined phase of nuclear matter in the high temperature regime, known as the quark-gluon plasma (QGP). In current heavy ion collision experiments, the QGP only lives for a short time period (roughly 10 fm/c in the laboratory frame) and we cannot directly measure its properties. Therefore, we use probes such as particle multiplicities and azimuthal distributions, jets and hadrons containing heavy quarks to indirectly study its properties. Various properties of the QGP are encoded in terms of gauge invariant correlation functions of field operators that often define transport coefficients showing up in the time evolution equations of the probes in the medium. Well-known examples include the shear viscosity (defined as a correlator of stress-energy tensors), the jet quenching parameter (a correlator of light-like Wilson lines) and the heavy quark diffusion coefficient (a correlator of two chromoelectric fields dressed with Wilson lines). Since the QGP is a strongly coupled fluid, nonperturbative determinations of these transport coefficients are crucial in our understanding of the QGP and QCD at finite temperature. Common nonperturbative methods include lattice QCD calculations and the holographic correspondence [1]. One can also extract these transport coefficients from experimental data by solving in-medium evolution equations (which can be model dependent) for different values of the transport coefficients and then performing a Bayesian analysis [2–6].

Recently, thanks to the advance in applying the open quantum system framework to study jets [7] and quarkonia [8–26] in the QGP (for recent reviews, see

Refs. [27–30]), a novel correlator of two chromoelectric fields dressed with Wilson lines that determines transport properties of quarkonium in the medium was constructed [12, 20]. This correlator for quarkonium transport is similar to but different from the correlator defining the heavy quark diffusion coefficient [31, 32] in terms of the ordering of the fields contained in the Wilson lines. Perturbative calculations in R_ξ gauge showed that the spectral function of the correlator for quarkonium transport [33] differs from that for heavy quark transport [34] by a temperature independent constant at next-to-leading order (NLO). However, if both calculations had been performed in temporal axial gauge ($A_0 = 0$), one would, at first sight, have concluded that the two correlators were identical. This resulted in a puzzle: Since both correlators are defined in a gauge invariant way, calculations with different gauge choices must give the same result. This puzzle was resolved in Ref. [35], establishing the difference between the two correlators on a more solid ground in QCD. Beyond NLO, the heavy quark diffusion coefficient has been studied by using hard-thermal-loop resummation [36], as well as nonperturbatively via the lattice QCD method [37–41] and the AdS/CFT correspondence [31, 42, 43]. On the other hand, a recent AdS/CFT calculation showed that the analog quarkonium transport coefficients in $\mathcal{N} = 4$ supersymmetric Yang-Mills (SYM) theory are zero [44], in stark contrast to the heavy quark diffusion coefficient value of $\sqrt{\lambda}\pi T^3$ at large coupling $\lambda = g^2 N_c \gg 1$. This difference is surprising because the heavy quark and quarkonium transport coefficients are defined by similar chromoelectric field correlators. Therefore, it is well motivated to study the quarkonium transport properties nonperturbatively in QCD. It is also crucial and urgent, since quarkonium production serves as an important probe of the QGP that is produced strongly coupled in current heavy ion collision experiments.

* bscheihi@mit.edu

† xjyao@uw.edu

In this article, we discuss how to extract the quarkonium transport coefficients from lattice QCD calculations of a specific Euclidean chromoelectric correlator. The paper is organized as follows: We will first review the quarkonium transport coefficients in the real-time formalism in Section II, which are defined in terms of a correlator of two chromoelectric fields connected via an adjoint Wilson line. Then, in Section III we will discuss the Euclidean version of the correlator and how to relate it to its real time counterpart. Next, in Section IV the setup of a lattice QCD calculation of this Euclidean correlator will be discussed, with a focus on how to renormalize it. Finally, we will conclude and present our outlook in Section V.

II. QUARKONIUM TRANSPORT PROPERTIES

The quarkonium transport coefficients are defined in terms of time-ordered chromoelectric field operators, dressed with Wilson lines [12]:

$$\begin{aligned}\kappa_{\text{adj}} &\equiv \frac{g^2 T_F}{3N_c} \text{Re} \int dt \langle \mathcal{T} E_i^a(t) W^{ab}(t, 0) E_i^b(0) \rangle_T \\ \gamma_{\text{adj}} &\equiv \frac{g^2 T_F}{3N_c} \text{Im} \int dt \langle \mathcal{T} E_i^a(t) W^{ab}(t, 0) E_i^b(0) \rangle_T,\end{aligned}\quad (1)$$

where $\langle O \rangle_T \equiv \text{Tr}(O e^{-\beta H}) / \text{Tr}(e^{-\beta H})$, E_i^a is a chromoelectric field, $W^{ab}(t, 0)$ denotes a time-like Wilson line in adjoint representation from $t = 0$ to t , \mathcal{T} represents the time-ordering symbol, $N_c = 3$ is the number of colors, and $T_F = 1/2$ is the normalization of the fundamental representation generator matrices. To simplify the notation we have neglected the spatial coordinates, which are the same for all the fields, and will do so throughout the paper, unless the spatial coordinates are no longer the same. Both κ_{adj} and γ_{adj} appear in the Lindblad equation describing the time evolution of a heavy quark-antiquark pair ($Q\bar{Q}$) at a small distance in the quantum Brownian motion limit [11, 12]:

$$\begin{aligned}\frac{d\rho_S(t)}{dt} &= -i[H_S + \gamma_{\text{adj}} \Delta h_S, \rho_S(t)] \\ &+ \kappa_{\text{adj}} (L_{\alpha i} \rho_S(t) L_{\alpha i}^\dagger - \frac{1}{2} \{L_{\alpha i}^\dagger L_{\alpha i}, \rho_S(t)\}),\end{aligned}\quad (2)$$

where ρ_S is the subsystem density matrix of the $Q\bar{Q}$ pair, $\gamma_{\text{adj}} \Delta h_S$ is the thermal correction to the vacuum $Q\bar{Q}$ Hamiltonian H_S and $L_{\alpha i}$ denotes the relevant Lindblad ‘‘jump’’ operators. Their explicit expressions are given in Appendix A. The κ_{adj} parameter in the non-Hermitian part of the Lindblad equation determines the rate of transition between a $Q\bar{Q}$ pair in the color singlet state and that in the color octet state, as well as wavefunction decoherence. On the other hand, the γ_{adj} parameter in the Hermitian part of the Lindblad equation controls the modification of the $Q\bar{Q}$ potential caused by the medium.

One way to interpret the integrations in Eq. (1) is as Fourier transforms that convert the time domain to

the frequency domain. Consequently, the coefficients κ_{adj} and γ_{adj} are the zero frequency limits of frequency-dependent correlation functions. Moreover, their behavior at finite frequency also turns out to be physically important. To explain the physical meaning of these correlation functions at finite frequency, we introduce path-ordered chromoelectric field correlators [20, 33]

$$\begin{aligned}[g_{\text{adj}}^{++}]^>(t) &\equiv \frac{g^2 T_F}{3N_c} \langle E_i^a(t) W^{ac}(t, +\infty) \\ &W^{cb}(+\infty, 0) E_i^b(0) \rangle_T \\ [g_{\text{adj}}^{--}]^>(t) &\equiv \frac{g^2 T_F}{3N_c} \langle W^{dc}(-i\beta - \infty, -\infty) W^{cb}(-\infty, t) \\ &E_i^b(t) E_i^a(0) W^{ad}(0, -\infty) \rangle_T,\end{aligned}\quad (3)$$

and consider their Fourier transforms $[g_{\text{adj}}^{\pm\pm}]^>(\omega) = \int dt e^{i\omega t} [g_{\text{adj}}^{\pm\pm}]^>(t)$. The path-ordered version is more convenient to use at finite frequency and is consistent with the time-ordered version: It has been shown that $\kappa_{\text{adj}} = [g_{\text{adj}}^{++}]^>(\omega = 0)$ [35]. The path-ordered correlators at finite frequency appear in the Boltzmann (rate) equation for quarkonium dissociation and recombination, which is derived in the quantum optical limit of the open quantum system approach [20, 33]:

$$\frac{dn_b(t, \mathbf{x})}{dt} = -\Gamma n_b(t, \mathbf{x}) + F(t, \mathbf{x}),\quad (4)$$

where Γ denotes the dissociation rate and F represents the formation of quarkonium from a recombining pair of unbound heavy quarks $Q\bar{Q}$

$$\Gamma = \frac{g^2 T_F}{3N_c} \int \frac{d^3 p_{\text{rel}}}{(2\pi)^3} |\langle \psi_b | \mathbf{r} | \Psi_{\mathbf{p}_{\text{rel}}} \rangle|^2 [g_E^{++}]^>(\Delta E)\quad (5)$$

$$\begin{aligned}F &= \frac{g^2 T_F}{3N_c} \int \frac{d^3 p_{\text{cm}}}{(2\pi)^3} \frac{d^3 p_{\text{rel}}}{(2\pi)^3} |\langle \psi_b | \mathbf{r} | \Psi_{\mathbf{p}_{\text{rel}}} \rangle|^2 \\ &\times [g_E^{--}]^>(\Delta E) f_{Q\bar{Q}}(t, \mathbf{x}, \mathbf{p}_{\text{cm}}, \mathbf{x}_{\text{rel}} = 0, \mathbf{p}_{\text{rel}}),\end{aligned}\quad (6)$$

where a nonzero energy difference between the bound and unbound states $\Delta E = p_{\text{rel}}^2/M + |E_b|$ determines how the finite frequency dependence of the correlators appears in the transition rates. Here M is the heavy quark mass. The transition occurs via a color dipole interaction $\langle \psi_b | \mathbf{r} | \Psi_{\mathbf{p}_{\text{rel}}} \rangle$ between a bound $Q\bar{Q}$ state $|\psi_b\rangle$ and an unbound scattering wave $|\Psi_{\mathbf{p}_{\text{rel}}}\rangle$. $f_{Q\bar{Q}}$ denotes the distribution of unbound heavy quark pairs with center-of-mass positions \mathbf{x} and momenta \mathbf{p}_{cm} and relative positions $\mathbf{x}_{\text{rel}} = 0$ and momenta \mathbf{p}_{rel} .

The chromoelectric field correlator for quarkonium transport is different from that for heavy quark diffusion. In particular, the heavy quark diffusion coefficient κ_{fund} and an analogous quantity γ_{fund} (whose physical meaning has not been explored for heavy quark transport) are

defined by

$$\begin{aligned}\kappa_{\text{fund}} &= \frac{g^2}{3N_c} \text{Re} \int dt \quad (7) \\ &\quad \langle \text{Tr}_c [U(-\infty, t) E_i(t) U(t, 0) E_i(0) U(0, -\infty)] \rangle_{T, Q}, \\ \gamma_{\text{fund}} &= \frac{g^2}{3N_c} \text{Im} \int dt \\ &\quad \langle \text{Tr}_c [U(-\infty, t) E_i(t) U(t, 0) E_i(0) U(0, -\infty)] \rangle_{T, Q},\end{aligned}$$

where $E_i = E_i^a T_F^a$ is the Lie algebra-valued chromoelectric field, with the fundamental representation generator matrices normalized as $\text{Tr}_c(T_F^a T_F^b) = T_F \delta^{ab}$. Also, Tr_c denotes trace over color indices and $U(t, 0)$ represents a time-like fundamental Wilson line from $t = 0$ to t . Here the subscript Q indicates the inclusion of the heavy quark effect in the thermal density matrix. In practical calculations, this leads to a fundamental Wilson line along the imaginary time at $t = -\infty$, which is explicit in the Euclidean setup presented in what follows. It is noted that the operators involved in the definition of κ_{fund} and γ_{fund} are path-ordered. We want to emphasize that the crucial difference between Eqs. (1) and (7) is not the representations of the Wilson lines, but the different orderings of the operators.

III. EUCLIDEAN CORRELATORS AND TRANSPORT COEFFICIENTS

As is well known, lattice QCD methods can only calculate correlation functions in Euclidean space and thus cannot be applied directly to study the real-time correlators defined in Eq. (3). In this section, we will introduce a Euclidean version of the correlator for quarkonium transport and discuss how to extract the quarkonium transport coefficients from the evaluation of this Euclidean correlator. As we will show, both the Euclidean correlator itself and the method to extract the quarkonium transport coefficients are different from the case of heavy quark diffusion in subtle and important aspects. To make the comparison more explicit, and also to take advantage of the apparent similarities between them, we will first review the extraction of the heavy quark diffusion coefficient from the corresponding Euclidean correlator.

A. Heavy Quark Diffusion

The Euclidean correlator relevant for the heavy quark diffusion case is given by [32]

$$G_{\text{fund}}(\tau) = -\frac{1}{3} \frac{\langle \text{ReTr}_c [U(\beta, \tau) g E_i(\tau) U(\tau, 0) g E_i(0)] \rangle_T}{\langle \text{ReTr}_c [U(\beta, 0)] \rangle_T}, \quad (8)$$

where $\beta = 1/T$ is the inverse of the QGP temperature and $\langle \cdot \rangle_T = \text{Tr}(e^{-\beta H}) / \text{Tr}(e^{-\beta H})$, with H the Hamiltonian of the QGP in the absence of any external color

source. It has been shown that the heavy quark transport coefficient can be obtained from $G_{\text{fund}}(\tau)$ via [32, 45]

$$\begin{aligned}\kappa_{\text{fund}} &= \lim_{\omega \rightarrow 0} \frac{T}{\omega} \rho_{\text{fund}}(\omega), \quad (9) \\ \gamma_{\text{fund}} &= -\int_0^\beta d\tau G_{\text{fund}}(\tau),\end{aligned}$$

where the spectral function $\rho_{\text{fund}}(\omega)$ is related to the Euclidean correlator through¹

$$G_{\text{fund}}(\tau) = \int_0^{+\infty} \frac{d\omega}{2\pi} \frac{\cosh(\omega(\tau - \frac{1}{2T}))}{\sinh(\frac{\omega}{2T})} \rho_{\text{fund}}(\omega). \quad (10)$$

This correlator is constructed such that the standard Kubo-Martin-Schwinger (KMS) and analytic continuation relations hold as in textbook thermal field theory. Given an analytic expression for $G_{\text{fund}}(\omega_n)$, with $\omega_n = 2\pi T n$, $n \in \mathbb{Z}$ the Matsubara frequencies, one can extract the spectral function by taking the real part² of the retarded correlator obtained by analytic continuation $\omega_n \rightarrow -i(\omega + i\epsilon)$ of this Euclidean correlator. This has been done both at weak [34] (QCD) and strong [31] ($\mathcal{N} = 4$ SYM) coupling. However, at physical values of the coupling in QCD, the only tool available at the moment is lattice gauge theory, and as such, the reconstruction of the spectral function ρ_{fund} through the relation (10) has received much attention in recent years [41, 46, 47].

Comparatively, the theoretical treatment of quarkonium transport coefficients has received less attention. We now aim to fill in this gap, and subsequently, to provide a recipe to determine these transport coefficients from lattice QCD calculations. To this end, we need to first construct a Euclidean version of the correlator for quarkonium transport that can be calculated via lattice QCD methods, and then explain how to extract the quarkonium transport coefficients from the evaluation of such an Euclidean correlator. We will answer these two questions in the following two subsections. Details of the lattice calculation of the Euclidean correlator will be discussed in the next section.

B. Euclidean Correlator for Quarkonium Transport

To construct the Euclidean correlator for quarkonium transport, we first note that because of the operator ordering in the definitions (3), we can equivalently write

$$[g_{\text{adj}}^{++}]^>(t) = \frac{g^2 T_F}{3N_c} \langle E_i^a(t) W^{ab}(t, 0) E_i^b(0) \rangle_T. \quad (11)$$

¹ Our convention for the Fourier transform is $O(\omega) = \int dt e^{i\omega t} O(t)$.

² Many studies define correlation functions with an imaginary unit prefactor, and there the spectral function corresponds to the imaginary part of the retarded correlator, which has a factor of 1/2 compared with the spectral function defined by the difference between the $>$ and $<$ Wightman correlators in frequency space.

To perform the analytic continuation, it is best to explicitly isolate the t dependence from the field operators and write it purely in terms of time evolution factors. We let H be the Hamiltonian of the thermal bath QGP in the absence of any external color charge. When an external adjoint color charge is present, the Hamiltonian of the thermal bath is given by $[H\mathbb{1} - gA_0^c(0)T_{\text{adj}}^c]^{ab}$. The reason for the appearance of this modified Hamiltonian can be seen from converting the adjoint Wilson line back to the Schrödinger picture from the interaction picture

$$e^{-iHt}W^{ab}(t,0) = \left[e^{-i(H-gA_0^c(0)T_{\text{adj}}^c)t} \right]^{ab}. \quad (12)$$

Eq. (12) has the following physical interpretation: during the time interval between 0 and t the QGP evolves in the presence of an adjoint color charge, which is manifest in the modification of the Hamiltonian by $-gA_0$. It is essentially a local modification to Gauss's law³, revealing the presence of a color octet $Q\bar{Q}$ pair. Outside this time interval the QGP evolves in the absence of external color sources.

Using Eq. (12), one can write:

$$\begin{aligned} & \frac{3N_c}{g^2T_F} [g_{\text{adj}}^{++}]^>(t) \\ &= \frac{\text{Tr}_{\mathcal{H}} \left[e^{iHt} E_i^a(0) \left[e^{-i(H-gA_0^c(0)T_{\text{adj}}^c)t} \right]^{ab} E_i^b(0) e^{-\beta H} \right]}{\text{Tr}_{\mathcal{H}} [e^{-\beta H}]}, \end{aligned} \quad (13)$$

where the trace $\text{Tr}_{\mathcal{H}}$ runs over physical states of the QGP. The analytic continuation is now direct, because all of the time dependence is in the exponentials. We just set $t \rightarrow -i\tau$, and identify the Euclidean gauge field A_4 with the Minkowski one by $A_0(0) = iA_4(0)$, to find

$$\begin{aligned} & [g_{\text{adj}}^{++}]^>(-i\tau) \\ &= \frac{g^2T_F}{3N_c} \frac{\text{Tr}_{\mathcal{H}} \left[e^{H\tau} E_i^a(0) \left[e^{-(H-gA_0^c(0)T_{\text{adj}}^c)\tau} \right]^{ab} E_i^b(0) e^{-\beta H} \right]}{\text{Tr}_{\mathcal{H}} [e^{-\beta H}]} \\ &= \frac{g^2T_F}{3N_c} \langle E_i^a(\tau) \left[\text{P exp} \left(ig \int_0^\tau d\tau' A_4^c(\tau') T_{\text{adj}}^c \right) \right]^{ab} E_i^b(0) \rangle_T \\ &= \frac{g^2T_F}{3N_c} \langle E_i^a(\tau) W^{ab}(\tau,0) E_i^a(0) \rangle_T \\ &\equiv G_{\text{adj}}(\tau). \end{aligned} \quad (14)$$

³ An interesting question one can ask of this expression is whether we still have explicit gauge invariance. The answer is, naturally, affirmative. However, this is not as easy to see when considering time-dependent gauge transformations as it is for time-independent gauge transformations. This is because the Hamiltonian also changes if one considers time-dependent gauge transformations, which is something to keep in mind when quantizing the theory. We will not pursue this further here, and we shall assume that H is already determined. For a thorough discussion on the quantization of gauge theories, we refer the reader to Ref. [48].

That is to say, we have proven that one of the real-time correlations we want to evaluate is related to an Euclidean correlation function by $[g_{\text{adj}}^{++}]^>(-i\tau) = G_{\text{adj}}(\tau)$. We note that the absence of the denominator term as in Eq. (8) is a result of the absence of a Wilson line along the imaginary time direction at $t = -\infty$ in the definition of $[g_{\text{adj}}^{++}]^>$. In quarkonium dissociation, the initial state is a color singlet, whereas in heavy quark diffusion, the initial state is in a color triplet representation, whose effect appears explicitly in the initial thermal state.

C. Extraction of Quarkonium Transport Coefficients from Euclidean QCD

Now we discuss how to extract the quarkonium transport coefficients from $G_{\text{adj}}(\tau)$. Even though this correlation function has been studied in the past [49–51], its precise connection to quarkonium transport has remained unexplored, until now. It turns out that neither Eq. (9) nor Eq. (10) is valid for the quarkonium case. This is so because Eq. (9) is a result of the standard KMS relation, which, as we will show momentarily, is more complicated for the quarkonium correlator. Furthermore, Eq. (10) relies on the spectral function being odd in ω , which is crucially not true for the correlators we will discuss in what follows.

1. KMS Relation and Non-odd Spectral Function

To explain the non-oddness of the spectral function for quarkonium transport, we follow Ref. [33] to use the usual proof of the KMS relation, plus the time-reversal operation and find

$$[g_{\text{adj}}^{++}]^>(\omega) = e^{\omega/T} [g_{\text{adj}}^{--}]^>(-\omega), \quad (15)$$

which is the necessary KMS relation for proper thermalization of the internal degrees of freedom of the heavy quark pair (their relative motion and internal quantum numbers [52]). We then introduce the spectral function that governs quarkonium transport as

$$\rho_{\text{adj}}^{++}(\omega) = [g_{\text{adj}}^{++}]^>(\omega) - [g_{\text{adj}}^{--}]^>(-\omega), \quad (16)$$

which, by definition satisfies $[g_{\text{adj}}^{++}]^>(\omega) = (1 + n_B(\omega))\rho_{\text{adj}}^{++}(\omega)$, with $n_B(\omega) = (e^{\beta\omega} - 1)^{-1}$. We have kept the superscripts “++” in the label of this spectral function because we can also define

$$\rho_{\text{adj}}^{--}(\omega) = [g_{\text{adj}}^{--}]^>(\omega) - [g_{\text{adj}}^{++}]^>(-\omega), \quad (17)$$

which contains the same information, and satisfies $\rho_{\text{adj}}^{--}(\omega) = -\rho_{\text{adj}}^{++}(-\omega)$.

We note that because of the explicit operator ordering, only in $[g_{\text{adj}}^{++}]^>$ the adjoint Wilson lines can be rewritten as $W^{ab}(t,0)$, which appears in the time-ordered correlator shown in Eq. (1). Furthermore, one can obtain the

time-ordered correlator that enters the definition of κ_{adj} and γ_{adj} by considering

$$\begin{aligned} [g_{\text{adj}}^{\mathcal{T}}](t) &\equiv \langle \mathcal{T} E_i^a(t) W^{ab}(t, 0) E_i^b(0) \rangle_T \\ &= \theta(t) [g_{\text{adj}}^{++}]^>(t) + \theta(-t) [g_{\text{adj}}^{++}]^>(-t). \end{aligned} \quad (18)$$

Here comes the most important part: The spectral function (16) is not odd in ω . In the standard thermal field theory setup, we define $\rho(\omega) = g^>(\omega) - g^<(\omega)$ where $g^>(t) = \langle \phi(t)\phi(0) \rangle$ and $g^<(t) = \langle \phi(0)\phi(t) \rangle$, which are related via $g^>(\omega) = g^<(-\omega)$ in frequency space by time translational invariance. This immediately leads to $\rho(\omega) = -\rho(-\omega)$. However, the relation $g^>(\omega) = g^<(-\omega)$ is not true for $[g_{\text{adj}}^{++}]^>(\omega)$ and $[g_{\text{adj}}^{--}]^>(\omega)$ due to the path ordering of field operators and the additional Wilson line along the imaginary time in $[g_{\text{adj}}^{--}]^>$. That is to say, $[g_{\text{adj}}^{--}]^>(t) \neq [g_{\text{adj}}^{++}]^>(t)$. Therefore, we do not know how $\rho_{\text{adj}}^{++}(\omega)$ transforms under $\omega \rightarrow -\omega$ a priori.

To see this more formally, one may also write the spectral function as a spectral decomposition in terms of the eigenvalues/eigenstates of H , denoted by $\{E_n, |n\rangle\}$, and those of $[H\mathbb{1} - gA_0^c(0)T_{\text{adj}}^c]^{ab}$, denoted by $\{\tilde{E}_n, |\tilde{n}^a\rangle\}$, where a is interpreted as a component of the state, rather than a label. With these definitions, it follows that

$$\begin{aligned} \rho_{\text{adj}}^{++}(\omega) &= \frac{g^2 T_F}{3N_c} \sum_{n, \tilde{n}} (2\pi) \delta(\omega + E_n - \tilde{E}_{\tilde{n}}) |\langle n | E_i^a(0) | \tilde{n}^a \rangle|^2 \\ &\quad \times \left[e^{-\beta E_n} - e^{-\beta \tilde{E}_{\tilde{n}}} \right]. \end{aligned} \quad (19)$$

There is no reason why this expression would be odd under $\omega \rightarrow -\omega$, because the energies E_n and \tilde{E}_n can (and will) be different in general.

Indeed, explicit perturbative calculations at NLO show that $\rho_{\text{adj}}^{++}(\omega)$ contains both ω -odd, which is the usual case, and ω -even parts (see Appendix B). The final result Eq. (3.66) shown in Ref. [33] is only for $\omega > 0$, as mentioned there. We have performed a similar calculation for $\omega < 0$ and found an ω -even part, which originates from the diagrams (5, 5r, 6 and 6r) of Ref. [33], or diagrams (j) of Refs. [34, 45]

$$\Delta\rho(\omega) \equiv (\rho_{\text{adj}}^{++}(\omega) - \rho_{\text{fund}}(\omega)) = \frac{g^4 T_F (N_c^2 - 1) \pi^2}{3(2\pi)^3} |\omega|^3, \quad (20)$$

where we have also added a factor of 2 since the definition of the spectral function shown in Eq. (3.66) of Ref. [33] differs from Eq. (16) by a factor of 2 (see Eq. (3.28) therein).

To demonstrate the importance of the ω -even part, we use it to recompute the difference between γ_{fund} and γ_{adj} at the order of α_s^2

$$\Delta\gamma \equiv \gamma_{\text{adj}} - \gamma_{\text{fund}} = -\frac{16\zeta(3)}{3} T_F C_F N_c \alpha_s^2 T^3, \quad (21)$$

where $C_F = \frac{N_c^2 - 1}{2N_c}$. This difference was first calculated in Ref. [45]. Some algebra and use of the definitions for

$[g_{\text{adj}}^{\pm\pm}]^>$ leads to

$$\begin{aligned} \gamma_{\text{adj}} &= \text{Im} \int_{-\infty}^{+\infty} dt (\theta(t) [g_{\text{adj}}^{++}]^>(t) + \theta(-t) [g_{\text{adj}}^{++}]^>(-t)) \\ \Delta\gamma &= -\frac{1}{\pi} \int_{-\infty}^{+\infty} \frac{d\omega}{|\omega|} (\theta(\omega) + n_B(|\omega|)) \Delta\rho(\omega), \end{aligned} \quad (22)$$

where we have used $[g_{\text{adj}}^{\pm\pm}]^>(\omega) = (1 + n_B(\omega)) \rho_{\text{adj}}^{\pm\pm}(\omega)$ and used that they are translationally invariant in time. The piece proportional to $\theta(\omega)$ is a pure vacuum contribution that vanishes in dimensional regularization. The second term inside the integral, however, gives a thermal contribution:

$$\begin{aligned} \Delta\gamma &= -\frac{4g^4 T_F}{3(2\pi)^4} \pi^2 (N_c^2 - 1) \int_0^{+\infty} \frac{\omega^2 d\omega}{e^{\omega/T} - 1} \\ &= -\frac{16\zeta(3)}{3} T_F C_F N_c \alpha_s^2 T^3, \end{aligned} \quad (23)$$

which is exactly the difference given in Eq. (21). This settles a long-standing issue regarding the consistency of the gauge-invariant chromoelectric correlators in adjoint and fundamental representation, and verifies explicitly that the spectral function relevant for quarkonium transport is qualitatively different from that for heavy quark diffusion. The above discrepancy $\Delta\gamma$ is explained precisely because $\rho_{\text{adj}}^{++}(\omega)$ is not odd in frequency.

With these theoretical foundations in hand, we can now proceed to write down the formula analogous to Eq. (10), which will allow for the extraction of κ_{adj} and γ_{adj} from the evaluation of the Euclidean correlator $G_{\text{adj}}(\tau)$.

2. Extraction Formulas

Using the fact that $G_{\text{adj}}(\tau)$ is the analytic continuation of $[g_{\text{adj}}^{++}]^>(t)$ to Euclidean signature, we can write

$$\begin{aligned} G_{\text{adj}}(\tau) &= \int_{-\infty}^{+\infty} \frac{d\omega}{2\pi} e^{-\omega\tau} [g_{\text{adj}}^{++}]^>(\omega) \\ &= \int_{-\infty}^{+\infty} \frac{d\omega}{2\pi} \frac{\exp(\omega(\frac{1}{2T} - \tau))}{2 \sinh(\frac{\omega}{2T})} \rho_{\text{adj}}^{++}(\omega). \end{aligned} \quad (24)$$

However, in contrast to Eq. (10), the integrand may not be symmetrized with respect to ω because $\rho_{\text{adj}}^{++}(\omega)$ is neither even nor odd. We note that, as one might suspect from Eq. (14) and is apparent from Eq. (24), the analytic continuation holds provided that $0 < \tau < \beta$. This is precisely the range where we discuss the calculation of G_{adj} in the next section. A direct calculation using

Eqs. (10), (20), and (24) shows that

$$\begin{aligned} \Delta G(\tau) &\equiv G_{\text{adj}}(\tau) - G_{\text{fund}}(\tau) \\ &= \int_{-\infty}^{+\infty} \frac{d\omega}{2\pi} \frac{\exp\left(\omega\left(\frac{1}{2T} - \tau\right)\right)}{2 \sinh\left(\frac{\omega}{2T}\right)} \Delta\rho(\omega) \\ &= \frac{g^4 T_F (N_c^2 - 1)}{(2\pi)^3} \pi T^4 [\zeta(4, \tau T) - \zeta(4, 1 - \tau T)] \\ &\quad + \mathcal{O}(g^6), \end{aligned} \quad (25)$$

where $\zeta(s, a) = \sum_{k=0}^{\infty} (k+a)^{-s}$ is the Hurwitz zeta function.

After extracting $\rho_{\text{adj}}^{++}(\omega)$ from the lattice QCD calculated $G_{\text{adj}}(\tau)$, which will be discussed in the next section, we can obtain κ_{adj} and γ_{adj} as

$$\begin{aligned} \kappa_{\text{adj}} &= \lim_{\omega \rightarrow 0} \frac{T}{2\omega} \left[\rho_{\text{adj}}^{++}(\omega) - \rho_{\text{adj}}^{++}(-\omega) \right] \\ \gamma_{\text{adj}} &= - \int_0^\beta d\tau G_{\text{adj}}(\tau) \\ &\quad - \frac{1}{2\pi} \int_{-\infty}^{+\infty} d\omega \frac{1 + 2n_B(|\omega|)}{|\omega|} \rho_{\text{adj}}^{++}(\omega), \end{aligned} \quad (26)$$

where the expression we have written for κ_{adj} makes it manifest that only the ω -odd part of $\rho_{\text{adj}}^{++}(\omega)$ contributes to it. (One can show this by using Eqs. (1) and (18).) We note that γ_{adj} may be substantially more difficult to extract than in the fundamental representation case. While the first term is indeed the same as in the fundamental case by virtue of $\int_{-\infty}^{+\infty} \frac{d\omega}{2\pi} \frac{\rho_{\text{adj}}^{++}(\omega)}{\omega} = \int_0^\beta d\tau G_{\text{adj}}(\tau)$, the fact that ρ_{adj}^{++} is not necessarily odd under $\omega \rightarrow -\omega$ means that the last term can contribute. Indeed, it does so in perturbation theory, as demonstrated by our calculation of $\Delta\gamma$ in Eq. (23). There is even an additional complication in that the 1 in $1 + 2n_B$ of the second line will usually generate ultraviolet divergences that have to be regulated analytically (e.g., by dimensional regularization). Furthermore, the first term may also require regularization for the integration regions where $\tau \approx 0, \beta$.

IV. LATTICE QCD DETERMINATION OF $G_{\text{adj}}(\tau)$ AND RENORMALIZATION

In this section, we discuss how to perform a lattice QCD calculation of G_{adj} and extract ρ_{adj}^{++} . We will first show a discretized version of G_{adj} and then discuss how to renormalize the lattice QCD result when taking the continuum limit. Finally we will give a fitting ansatz to extract ρ_{adj}^{++} from the calculated G_{adj} , which can then be plugged into Eq. (26) to obtain the quarkonium transport coefficients.

A. Lattice Discretization

The main ingredient we require in order to construct a lattice formulation of the correlator that determines

quarkonium transition rates is a discretized formula for the gauge field strength $F_{\mu\nu} = \partial_\mu A_\nu - \partial_\nu A_\mu - ig[A_\mu, A_\nu]$ in terms of link variables $U_\mu(n) = \exp(igaA_\mu(n))$:

$$\begin{aligned} [\Delta U]_{\mu\nu}(n) &= U_{-\nu}(n + \hat{\nu}) U_{-\mu}(n + \hat{\mu} + \hat{\nu}) U_\nu(n + \hat{\mu}) \\ &\quad \times U_\nu(n + \hat{\mu} - \hat{\nu}) U_\mu(n - \hat{\nu}) U_{-\nu}(n) - 1 \\ &= 2iga^2 F_{\mu\nu}(n) + \mathcal{O}(a^3). \end{aligned} \quad (27)$$

This discretization is different from the standard square plaquette. We chose this one because it makes the operator symmetric around the Wilson line direction, as shown in Fig. 1. One can then write an expression purely in terms of link variables for the correlator:

$$\begin{aligned} G_{\text{adj}}(\tau; a) &= \frac{(-1)}{12a^4 N_c} \left\langle \text{Tr}_c \left\{ \left(\prod_{n=n_\tau-1}^0 U_0^\dagger(n) \right) [\Delta U]_{\tau i}(n_\tau) \right. \right. \\ &\quad \left. \left. \times \left(\prod_{n=0}^{n_\tau-1} U_0(n) \right) [\Delta U]_{(-\tau)(-i)}(0) \right\} \right\rangle_E, \end{aligned} \quad (28)$$

where $\tau = an_\tau$, and the products are ordered in such a way that the lower limit of the index labels corresponds to the operator that is most to the right in the product, and the upper limit to the one that is most to the left. A graphic representation of the correlator can be found in Fig. 1. The average $\langle \cdot \rangle_E$ represents the expectation value under the measure defined by the Euclidean lattice path integral, i.e., $\langle O \rangle_E = \frac{1}{Z_E} \int DU \exp(-S_E[U]) O[U]$ where $Z_E = \int DU \exp(-S_E[U])$.

B. Renormalization and Infrared Renormalon

The bare chromoelectric correlator $G_{\text{adj}}(\tau; a)$ can be evaluated by the lattice method explained above. For physical quantities, the lattice calculation result needs proper renormalization. Since the operator involves a Wilson line, it is expected that $G_{\text{adj}}(\tau; a)$ contains a linear divergence (which has not been explicitly checked and should be done so in the future via, e.g., a perturbative calculation with a regularization method other than dimensional regularization), in addition to the usual logarithmic divergence. Therefore, we renormalize the bare correlator via

$$G_{\text{adj}}^R(\tau, \mu) = Z e^{\delta m \cdot \tau} G_{\text{adj}}(\tau; a), \quad (29)$$

where Z stands for the renormalization factor for the logarithmic divergence of the composite operator, with μ the renormalization scale and δm the mass renormalization associated with the self energy of the Wilson line. It has been shown that with this form of the renormalization factor for the nonlocal operator, one no longer needs to consider the effects of operator mixing in the renormalization group flow when one expresses this nonlocal operator on the lattice as a weighted sum of local lattice operators [53].

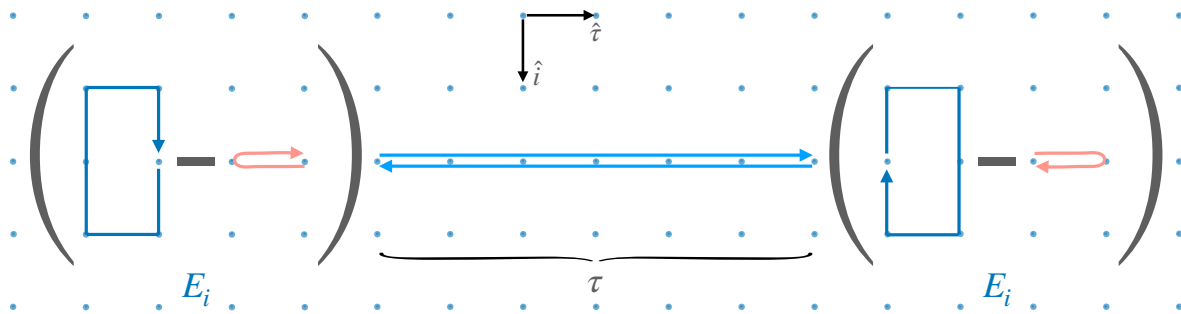


FIG. 1: Lattice discretization of the chromoelectric field correlator. The electric field insertions are constructed by taking the difference between the products of gauge links over the blue and red contours at the ends of the light blue contours, which represents an adjoint Wilson line. In this setup, the adjoint Wilson line is equivalent to two antiparallel fundamental Wilson lines.

A NLO calculation of the real-time partner of G_{adj} , i.e., $[g_{\text{adj}}^{++}]^>$ has shown that [33]

$$Z' = 1 + \frac{0}{\epsilon} + \text{finite terms at } g^2 + \mathcal{O}(g^4), \quad (30)$$

where we used Z' to distinguish the renormalization factor for $[g_{\text{adj}}^{++}]^>$ from the Z for G_{adj} . The “0” coefficient of the $1/\epsilon$ term emphasizes that $[g_{\text{adj}}^{++}]^>$ has no logarithmic divergence at NLO. The calculation was performed in the continuum by using dimensional regularization. The divergent term should be the same in the dimensionally regularized and lattice regularized perturbative calculations. Only the finite terms can be different. If we want to obtain the renormalized result in the $\overline{\text{MS}}$ scheme, the finite difference between the lattice scheme result and the $\overline{\text{MS}}$ result should still be accounted for. In the case of G_{fund} , the difference is known at NLO [54]. We leave the calculations of Z for the Euclidean G_{adj} in both schemes to future studies. (As can be seen by comparing to Ref. [54], such calculations are research projects on their own.)

Since the δm term is associated with the self energy of the Wilson line, one can use lattice perturbative calculations to determine it, but the uncertainties are expected to be large due to infrared renormalons. In particular, δm is expected to be of the form

$$\delta m = \frac{m_{-1}}{a} + m_0, \quad (31)$$

where m_0 is independent of the lattice spacing a . The infrared renormalon ambiguity leads to an uncertainty in summing the perturbative series for m_{-1} , which is compensated by the same uncertainty in determining m_0 . So we expect both m_{-1} and m_0 to be scheme dependent, as shown in the recent study on renormalizing the quasi parton distribution function (quasi-PDF) [55].

Here we discuss a strategy to reduce the uncertainty caused by the infrared renormalons in determining the renormalization factor δm by using lattice QCD calculation results, which is motivated by the recent work on self renormalization of the quark quasi-PDF [55, 56].

The first step is to fit m_{-1} from the a dependence of $G_{\text{adj}}(\tau; a)$ when a is small for each τ (we need to maintain $\tau \gg a$ to have negligible lattice artifacts). Then we define $G_{\text{adj}}^{R'}(\tau, \mu) \equiv Z e^{m_{-1}\tau/a} G_{\text{adj}}(\tau; a)$, i.e., we only absorb the extracted a -dependent linear divergence and the logarithmic divergence into the renormalization factor and perform an operator production expansion (OPE) at small τ (i.e., $\beta \gg \tau$ but we still require $\tau \gg a$)

$$G_{\text{adj}}^{R'}(\tau, \mu) = e^{-m_0\tau} \sum_n C_n(\alpha_s(\mu), \mu\tau) \tau^n \langle O_n \rangle_T^R(\mu) \quad (32)$$

$$\xrightarrow{\tau \rightarrow 0} (1 - m_0\tau) \sum_{n=0,1} C_n \tau^n \langle O_n \rangle_T^R + \mathcal{O}(\tau^2),$$

where O_n denotes the local operators in the OPE and $\langle O_n \rangle_T^R(\mu)$ represents their renormalized expectation values at the same temperature T . The expectation values of O_n can be calculated by standard lattice QCD methods and renormalized perturbatively by calculating the corresponding logarithmic renormalization factors via lattice perturbative calculations, in the same way as it is done for the logarithmic renormalization factor Z for G_{adj} . These local operators do not involve Wilson lines and thus do not have linear divergence, so it is expected that their renormalization is insensitive to the effects from infrared renormalons. The local OPE operators that may contribute include

$$\begin{aligned} O_0 &: \mathbb{1}, \text{Tr}_c(F_{0i}F_{0i}), \text{Tr}_c(F_{ij}F_{ij}), m_q \bar{q}q \\ O_1 &: e_\rho \text{Tr}_c(F_{0i}D^\rho F_{0i}), e_\rho \text{Tr}_c(F_{ij}D^\rho F_{ij}), e_\rho m_q \bar{q}D^\rho q, \end{aligned} \quad (33)$$

where e_ρ is a unit vector along the spacetime direction ρ . The short-distance Wilson coefficients C_n can be calculated in perturbation theory at the scale $\mu = 1/\tau$. The calculation of these coefficients is an active area of research [57, 58]. In practice, we can determine m_0 via Eq. (32) by calculating the lattice renormalized $G_{\text{adj}}^{R'}(\tau, \mu)$ and $\langle O_n \rangle_T^R(\mu)$. With m_0 determined, we can obtain $G_{\text{adj}}^R(\tau, \mu)$ from $G_{\text{adj}}^{R'}(\tau, \mu)$ by including the renormalization factor associated with m_0 . As suggested in Ref. [56],

to reduce the uncertainty caused by the infrared renormalons, one resums the leading infrared renormalons in C_n by regulating the renormalon poles in the Borel space and applying the inverse Borel transformation. As shown therein, this strategy removes a large uncertainty in the determination of the quark PDF. We expect a similar uncertainty reduction to happen for the determination of G_{adj}^R by using this strategy.

After determining the renormalized G_{adj}^R in the lattice regularization, we can convert it into the $\overline{\text{MS}}$ scheme if we know the difference between perturbative results in these two schemes.

C. Fitting Ansatz for ρ_{adj}^{++}

Once we obtain the renormalized G_{adj}^R , we can use Eq. (24) to fit the spectral function ρ_{adj}^{++} . Since we only have a limited number of data points in τ , we need a fitting ansatz. One ansatz that has been used in the lattice studies of the heavy quark diffusion coefficient is of the form [46]

$$\rho_{\text{adj}}^{++}(\omega) = \sqrt{\rho_{\text{IR}}^2(\omega) + \rho_{\text{UV}}^2(\omega)}, \quad (34)$$

where ρ_{IR} and ρ_{UV} represent ansatzes in the small and large ω regions, respectively. We will construct ansatzes motivated from perturbative studies.

The large frequency behavior of $\rho_{\text{adj}}^{++}(\omega)$ is determined by Eq. (20) and $\rho_{\text{fund}}(\omega)$, which may be read off from Ref. [34]. Explicitly,

$$\rho_{\text{adj}}^{++}(\omega) \stackrel{\omega \gg T}{\approx} \frac{g^2 T_F (N_c^2 - 1) \omega^3}{3(2\pi) N_c} \times \quad (35)$$

$$\left\{ 1 + \frac{g^2}{(2\pi)^2} \left[\left(\frac{11N_c}{12} - \frac{N_f}{6} \right) \ln \left(\frac{\mu^2}{4\omega^2} \right) + N_c \left(\frac{149}{36} - \frac{2\pi^2}{3} + \pi^2 \text{sgn}(\omega) \right) - \frac{5N_f}{9} \right] \right\}$$

$$+ \mathcal{O}(g^6),$$

where N_f is the number of light (massless) quark flavors in the theory. It was shown in Ref. [34] that up to $\mathcal{O}(g^4)$, the leading temperature-dependent contributions at large frequency go as T^4/ω .

On the infrared side, one needs to use the hard thermal loop effective theory to capture the behavior of correlation functions when $|\omega| \lesssim gT \propto m_D$, where m_D is the so-called Debye mass of the QGP, given (perturbatively) by $m_D^2 = g^2 T^2 \left(\frac{N_c}{3} + \frac{N_f}{6} \right)$, which quantifies color-electric screening in a thermal plasma. To see the difference between the ρ_{fund} and ρ_{adj} in the small ω region, one needs to consider the same type of diagram that led to the difference shown in Eq. (20), which has a prefactor of g^4 , meaning that the dominant corrections in the regime $|\omega| \lesssim m_D$ will be of order $g^4 m_D^2 |\omega| \propto g^6 T^2 |\omega|$. This means that we cannot make quantitative statements by

considering only the 1-loop diagram that leads to Eq. (20) (replacing the propagators with their HTL-resummed counterparts), as we can get competing effects from 2-loop diagrams in QCD, which contribute at order g^6 . In practice, one would also need to calculate these 2-loop diagrams to be able to match the HTL result to full QCD. We will leave such calculations to future studies. Here we only list the leading contribution in the infrared regime, which can be written in terms of the well-known heavy quark diffusion coefficient κ_{fund} at NLO:

$$\rho_{\text{adj}}^{++}(\omega) \stackrel{\omega \ll gT}{\approx} \rho_{\text{fund}}(\omega) \stackrel{\omega \ll gT}{\approx} \frac{\kappa_{\text{fund}} \omega}{T} + \mathcal{O}(g^6), \quad (36)$$

where κ_{fund} is given by [36, 59]:

$$\kappa_{\text{fund}} = \frac{g^4 T_F (N_c^2 - 1) T^3}{9(2\pi) N_c} \times \quad (37)$$

$$\left[\left(N_c + \frac{N_f}{2} \right) \left(\ln \frac{2T}{m_D} + \frac{1}{2} - \gamma_E + \frac{\zeta'(2)}{\zeta(2)} \right) + \frac{N_f}{2} \ln 2 + \frac{N_c m_D}{T} C \right] + \mathcal{O}(g^6),$$

with $C \approx 2.3302$, as given in Ref. [59]. The fact that the low-frequency limit of the adjoint and fundamental correlators do not differ up to this order had already been noticed in Ref. [59].

Motivated by the above perturbative analyzes, we suggest to use Eq. (35) as ρ_{UV} in the fitting ansatz (34) and use $\kappa_{\text{adj}} \omega + c|\omega|$ to parametrize ρ_{IR} with c some constant that does not contribute to κ_{adj} . The appearance of the $c|\omega|$ term in ρ_{IR} is a crucial difference from the case of the heavy quark diffusion coefficient and is motivated by perturbative calculations shown in Section III C 1. The fitting of ρ_{adj}^{++} will not only provide the quarkonium transport coefficient κ_{adj} , but also the frequency dependence of ρ_{adj}^{++} , which is important to evaluate γ_{adj} , as well as the frequency-dependent correlator $g_{\text{adj}}^{\pm\pm}(\omega)$ that determines the quarkonium dissociation and recombination rates.

V. CONCLUSIONS

In this paper, we explained how to determine the real time quarkonium transport properties from a Euclidean chromoelectric field correlator. This determination requires to reconstruct a spectral function in a way that is different from more intensively studied spectral function reconstruction problems, such as the one required for the extraction of the heavy quark diffusion coefficient. The key results are shown in Eq. (26). We then discussed the lattice determination of the Euclidean correlator, and in particular, a method to reduce the uncertainty caused by infrared renormalons in obtaining the renormalization factor for the linear divergence of the correlator. This method is quite involved and several perturbative calculations needed to implement the method are left to future studies, such

as the lattice-regularized perturbative calculation of the logarithmic renormalization factor Z in Eq. (29) and the Borel-resummed calculation of the Wilson coefficients in the OPE (32). Our work paves a way towards a non-perturbative determination of the quarkonium transport properties in the QCD hot medium, which generalizes the use of a weakly interacting gas of quarks and gluons as a microscopic model of the QGP in Boltzmann (rate) equations [60–63] for quarkonium to the strongly coupled case. This not only deepens our understanding of the QGP and quarkonium production in heavy ion collisions, but may also provide insights for studies of exotic heavy flavor production [64–66] and dark matter bound state formation in the early universe [33, 67–69].

ACKNOWLEDGMENTS

We thank Xiangdong Ji, Yin Lin, Peter Petreczky, Krishna Rajagopal, Martin J. Savage, Phiala E. Shanahan and Iain W. Stewart for useful discussions. We thank the Institute for Nuclear Theory (INT) at the University of Washington for its kind hospitality and stimulating research environment, and the organizers of the INT-22-3 program “Heavy Flavor Production in Heavy-Ion and Elementary Collisions”. This research was supported in part by the INT’s U.S. Department of Energy grant No. DE-FG02-00ER41132. B.S. is supported by the U.S. Department of Energy, Office of Science, Office of Nuclear Physics under grant Contract Number DE-SC0011090. X.Y. also acknowledges support from the U.S. Department of Energy, Office of Science, Office of Nuclear Physics, InQubator for Quantum Simulation (IQUS) under Award Number DOE (NP) Award DE-SC0020970.

-
- [1] J. Casalderrey-Solana, H. Liu, D. Mateos, K. Rajagopal, and U. A. Wiedemann, *Gauge/String Duality, Hot QCD and Heavy Ion Collisions* (Cambridge University Press, 2014) arXiv:1101.0618 [hep-th].
 - [2] J. E. Bernhard, J. S. Moreland, and S. A. Bass, *Nature Phys.* **15**, 1113 (2019).
 - [3] G. Nijs, W. van der Schee, U. Gürsoy, and R. Snellings, *Phys. Rev. Lett.* **126**, 202301 (2021), arXiv:2010.15130 [nucl-th].
 - [4] G. Nijs, W. van der Schee, U. Gürsoy, and R. Snellings, *Phys. Rev. C* **103**, 054909 (2021), arXiv:2010.15134 [nucl-th].
 - [5] D. Everett *et al.* (JETSCAPE), *Phys. Rev. C* **103**, 054904 (2021), arXiv:2011.01430 [hep-ph].
 - [6] S. Cao *et al.* (JETSCAPE), *Phys. Rev. C* **104**, 024905 (2021), arXiv:2102.11337 [nucl-th].
 - [7] V. Vaidya and X. Yao, *JHEP* **10**, 024 (2020), arXiv:2004.11403 [hep-ph].
 - [8] Y. Akamatsu and A. Rothkopf, *Phys. Rev. D* **85**, 105011 (2012), arXiv:1110.1203 [hep-ph].
 - [9] Y. Akamatsu, *Phys. Rev. D* **91**, 056002 (2015), arXiv:1403.5783 [hep-ph].
 - [10] R. Katz and P. B. Gossiaux, *Annals Phys.* **368**, 267 (2016), arXiv:1504.08087 [quant-ph].
 - [11] N. Brambilla, M. A. Escobedo, J. Soto, and A. Vairo, *Phys. Rev. D* **96**, 034021 (2017), arXiv:1612.07248 [hep-ph].
 - [12] N. Brambilla, M. A. Escobedo, J. Soto, and A. Vairo, *Phys. Rev. D* **97**, 074009 (2018), arXiv:1711.04515 [hep-ph].
 - [13] J.-P. Blaizot and M. A. Escobedo, *JHEP* **06**, 034 (2018), arXiv:1711.10812 [hep-ph].
 - [14] S. Kajimoto, Y. Akamatsu, M. Asakawa, and A. Rothkopf, *Phys. Rev. D* **97**, 014003 (2018), arXiv:1705.03365 [nucl-th].
 - [15] J.-P. Blaizot and M. A. Escobedo, *Phys. Rev. D* **98**, 074007 (2018), arXiv:1803.07996 [hep-ph].
 - [16] X. Yao and T. Mehen, *Phys. Rev. D* **99**, 096028 (2019), arXiv:1811.07027 [hep-ph].
 - [17] Y. Akamatsu, M. Asakawa, S. Kajimoto, and A. Rothkopf, *JHEP* **07**, 029 (2018), arXiv:1805.00167 [nucl-th].
 - [18] T. Miura, Y. Akamatsu, M. Asakawa, and A. Rothkopf, *Phys. Rev. D* **101**, 034011 (2020), arXiv:1908.06293 [nucl-th].
 - [19] R. Sharma and A. Tiwari, *Phys. Rev. D* **101**, 074004 (2020), arXiv:1912.07036 [hep-ph].
 - [20] X. Yao and T. Mehen, *JHEP* **02**, 062 (2021), arXiv:2009.02408 [hep-ph].
 - [21] Y. Akamatsu, M. Asakawa, and S. Kajimoto, *Phys. Rev. D* **105**, 054036 (2022), arXiv:2108.06921 [nucl-th].
 - [22] N. Brambilla, M. A. Escobedo, M. Strickland, A. Vairo, P. Vander Griend, and J. H. Weber, *Phys. Rev. D* **104**, 094049 (2021), arXiv:2107.06222 [hep-ph].
 - [23] T. Miura, Y. Akamatsu, M. Asakawa, and Y. Kaida, *Phys. Rev. D* **106**, 074001 (2022), arXiv:2205.15551 [nucl-th].
 - [24] N. Brambilla, M. A. Escobedo, A. Islam, M. Strickland, A. Tiwari, A. Vairo, and P. Vander Griend, *JHEP* **08**, 303 (2022), arXiv:2205.10289 [hep-ph].
 - [25] Z. Xie and B. Chen, (2022), arXiv:2205.13302 [nucl-th].
 - [26] H. Alalawi, J. Boyd, C. Shen, and M. Strickland, *Physical Review C* **107**, L031901 (2023).
 - [27] A. Rothkopf, *Phys. Rept.* **858**, 1 (2020), arXiv:1912.02253 [hep-ph].
 - [28] Y. Akamatsu, *Prog. Part. Nucl. Phys.* **123**, 103932 (2022), arXiv:2009.10559 [nucl-th].
 - [29] R. Sharma, *Eur. Phys. J. ST* **230**, 697 (2021), arXiv:2101.04268 [hep-ph].
 - [30] X. Yao, *Int. J. Mod. Phys. A* **36**, 2130010 (2021), arXiv:2102.01736 [hep-ph].
 - [31] J. Casalderrey-Solana and D. Teaney, *Phys. Rev. D* **74**, 085012 (2006), arXiv:hep-ph/0605199.
 - [32] S. Caron-Huot, M. Laine, and G. D. Moore, *JHEP* **04**, 053 (2009), arXiv:0901.1195 [hep-lat].

- [33] T. Binder, K. Mukaida, B. Scheiing-Hitschfeld, and X. Yao, *JHEP* **01**, 137 (2022), [arXiv:2107.03945 \[hep-ph\]](#).
- [34] Y. Burnier, M. Laine, J. Langelage, and L. Mether, *JHEP* **08**, 094 (2010), [arXiv:1006.0867 \[hep-ph\]](#).
- [35] B. Scheiing-Hitschfeld and X. Yao, *Phys. Rev. Lett.* **130**, 052302 (2023), [arXiv:2205.04477 \[hep-ph\]](#).
- [36] S. Caron-Huot and G. D. Moore, *Phys. Rev. Lett.* **100**, 052301 (2008), [arXiv:0708.4232 \[hep-ph\]](#).
- [37] D. Banerjee, S. Datta, R. Gavai, and P. Majumdar, *Phys. Rev. D* **85**, 014510 (2012), [arXiv:1109.5738 \[hep-lat\]](#).
- [38] H. T. Ding, A. Francis, O. Kaczmarek, F. Karsch, H. Satz, and W. Soeldner, *Phys. Rev. D* **86**, 014509 (2012), [arXiv:1204.4945 \[hep-lat\]](#).
- [39] A. Francis, O. Kaczmarek, M. Laine, T. Neuhaus, and H. Ohno, *Phys. Rev. D* **92**, 116003 (2015), [arXiv:1508.04543 \[hep-lat\]](#).
- [40] N. Brambilla, V. Leino, P. Petreczky, and A. Vairo, *Phys. Rev. D* **102**, 074503 (2020), [arXiv:2007.10078 \[hep-lat\]](#).
- [41] L. Altenkort, A. M. Eller, O. Kaczmarek, L. Mazur, G. D. Moore, and H.-T. Shu, *Phys. Rev. D* **103**, 014511 (2021), [arXiv:2009.13553 \[hep-lat\]](#).
- [42] C. P. Herzog, A. Karch, P. Kovtun, C. Kozcaz, and L. G. Yaffe, *JHEP* **07**, 013 (2006), [arXiv:hep-th/0605158](#).
- [43] S. S. Gubser, *Phys. Rev. D* **76**, 126003 (2007), [arXiv:hep-th/0611272](#).
- [44] G. Nijs, B. Scheiing-Hitschfeld, and X. Yao, (2023), [arXiv:2304.03298 \[hep-ph\]](#).
- [45] A. M. Eller, J. Ghiglieri, and G. D. Moore, *Phys. Rev. D* **99**, 094042 (2019), [Erratum: *Phys.Rev.D* 102, 039901 (2020)], [arXiv:1903.08064 \[hep-ph\]](#).
- [46] L. Altenkort, O. Kaczmarek, R. Larsen, S. Mukherjee, P. Petreczky, H.-T. Shu, and S. Stendebach, (2023), [arXiv:2302.08501 \[hep-lat\]](#).
- [47] N. Brambilla, V. Leino, J. Mayer-Stuedte, and P. Petreczky (TUMQCD), *Phys. Rev. D* **107**, 054508 (2023), [arXiv:2206.02861 \[hep-lat\]](#).
- [48] M. Henneaux and C. Teitelboim, *Quantization of gauge systems* (1992).
- [49] M. Eidemuller and M. Jamin, *Phys. Lett. B* **416**, 415 (1998), [arXiv:hep-ph/9709419](#).
- [50] M. Eidemuller, H. G. Dosch, and M. Jamin, *Nucl. Phys. B Proc. Suppl.* **86**, 421 (2000), [arXiv:hep-ph/9908318](#).
- [51] M. D'Elia, A. Di Giacomo, and E. Meggiolaro, *Phys. Rev. D* **67**, 114504 (2003), [arXiv:hep-lat/0205018](#).
- [52] X. Yao and B. Müller, *Phys. Rev. C* **97**, 014908 (2018), [Erratum: *Phys.Rev.C* 97, 049903 (2018)], [arXiv:1709.03529 \[hep-ph\]](#).
- [53] B. U. Musch, P. Hagler, J. W. Negele, and A. Schafer, *Phys. Rev. D* **83**, 094507 (2011), [arXiv:1011.1213 \[hep-lat\]](#).
- [54] C. Christensen and M. Laine, *Phys. Lett. B* **755**, 316 (2016), [arXiv:1601.01573 \[hep-lat\]](#).
- [55] Y.-K. Huo *et al.* (Lattice Parton Collaboration (LPC)), *Nucl. Phys. B* **969**, 115443 (2021), [arXiv:2103.02965 \[hep-lat\]](#).
- [56] R. Zhang, J. Holligan, X. Ji, and Y. Su, (2023), [arXiv:2305.05212 \[hep-lat\]](#).
- [57] V. M. Braun, K. G. Chetyrkin, and B. A. Kniehl, *JHEP* **07**, 161 (2020), [arXiv:2004.01043 \[hep-ph\]](#).
- [58] V. M. Braun, K. G. Chetyrkin, and B. A. Kniehl, *JHEP* **05**, 231 (2021), [arXiv:2103.09478 \[hep-ph\]](#).
- [59] S. Caron-Huot and G. D. Moore, *JHEP* **02**, 081 (2008), [arXiv:0801.2173 \[hep-ph\]](#).
- [60] R. Rapp and X. Du, *Nucl. Phys. A* **967**, 216 (2017), [arXiv:1704.07923 \[hep-ph\]](#).
- [61] X. Yao and B. Müller, *Phys. Rev. D* **100**, 014008 (2019), [arXiv:1811.09644 \[hep-ph\]](#).
- [62] X. Du, S. Y. F. Liu, and R. Rapp, *Phys. Lett. B* **796**, 20 (2019), [arXiv:1904.00113 \[nucl-th\]](#).
- [63] X. Yao, W. Ke, Y. Xu, S. A. Bass, and B. Müller, *JHEP* **01**, 046 (2021), [arXiv:2004.06746 \[hep-ph\]](#).
- [64] X. Yao and B. Müller, *Phys. Rev. D* **97**, 074003 (2018), [arXiv:1801.02652 \[hep-ph\]](#).
- [65] B. Wu, Z. Tang, M. He, and R. Rapp, (2022), [arXiv:2209.13795 \[hep-ph\]](#).
- [66] B. Wu, Z. Tang, M. He, and R. Rapp, (2023), [arXiv:2302.11511 \[nucl-th\]](#).
- [67] T. Binder, B. Blobel, J. Harz, and K. Mukaida, *JHEP* **09**, 086 (2020), [arXiv:2002.07145 \[hep-ph\]](#).
- [68] S. Biondini, T. A. Chowdhury, and S. Saad, (2023), [arXiv:2306.09428 \[hep-ph\]](#).
- [69] S. Biondini, N. Brambilla, G. Qerimi, and A. Vairo, (2023), [arXiv:2304.00113 \[hep-ph\]](#).
- [70] J. O. Andersen, E. Braaten, E. Petitgirard, and M. Strickland, *Phys. Rev. D* **66**, 085016 (2002), [arXiv:hep-ph/0205085](#).

Appendix A: Detailed Expressions in the Lindblad Equation

Here we write out explicitly each term in the Lindblad equation (2) introduced in the main text, which can be found in the literature, e.g., in Ref. [24]. The density matrix is assumed to be block diagonal in the color singlet and octet basis

$$\rho_S(t) = \begin{pmatrix} \rho_S^{(s)}(t) & 0 \\ 0 & \rho_S^{(o)}(t) \end{pmatrix}. \quad (\text{A1})$$

The Hamiltonian and its thermal correction are given by [$C_F = (N_c^2 - 1)/(2N_c)$]

$$H_S = \frac{\mathbf{p}_{\text{rel}}^2}{M} + \begin{pmatrix} -\frac{C_F \alpha_s}{r} & 0 \\ 0 & \frac{\alpha_s}{2N_c r} \end{pmatrix}, \quad \gamma_{\text{adj}} \Delta h_S = \frac{\gamma_{\text{adj}}}{2} r^2 \begin{pmatrix} 1 & 0 \\ 0 & \frac{N_c^2 - 2}{2(N_c^2 - 1)} \end{pmatrix}, \quad (\text{A2})$$

The Lindblad operators are given by

$$\begin{aligned} L_{1i} &= \left(r_i + \frac{1}{2MT} \nabla_i - \frac{N_c \alpha_s r_i}{8T r} \right) \begin{pmatrix} 0 & 0 \\ 1 & 0 \end{pmatrix} \\ L_{2i} &= \sqrt{\frac{1}{N_c^2 - 1}} \left(r_i + \frac{1}{2MT} \nabla_i + \frac{N_c \alpha_s r_i}{8T r} \right) \begin{pmatrix} 0 & 1 \\ 0 & 0 \end{pmatrix} \\ L_{3i} &= \sqrt{\frac{N_c^2 - 4}{2(N_c^2 - 1)}} \left(r_i + \frac{1}{2MT} \nabla_i \right) \begin{pmatrix} 0 & 0 \\ 0 & 1 \end{pmatrix}, \end{aligned} \quad (\text{A3})$$

where $i = x, y, z$.

Appendix B: Calculation Details of Spectral Function Difference

As explained in the main text, the difference between the spectral function for quarkonium transport and that for single heavy quark transport is given by the diagrams (j) in Refs. [34, 45], or (5), (5r) in Ref. [33]. The diagrammatic representation of their difference in real time in terms of Wightman functions was given in Ref. [35], where gauge invariance was also examined.

Following the calculation details of Ref. [33], we find that the difference between these two spectral functions is given by

$$\begin{aligned} \rho_{\text{adj}}^{++}(\omega) - \rho_{\text{fund}}(\omega) &= \int_{\mathbf{p}, k} \frac{T_F}{3N_c} g^4 N_c (N_c^2 - 1) 2\pi \delta(k_0) [g_{\mu\nu} (p - 2k)_\delta + g_{\nu\delta} (k - 2p)_\mu + g_{\delta\mu} (p + k)_\nu] \\ &\quad \times (p_0 g_{i\delta'} - p_i g_{0\delta'}) ((p_0 - k_0) g_{i\nu'} - (p_i - k_i) g_{0\nu}) \\ &\quad \times \text{Re} \left\{ [\rho(p)]^{\delta'\delta} [D_T(p - k)]^{\nu\nu'} [D_T(k)]^{\mu 0} \right. \\ &\quad \left. - [D_T(p)]^{\delta'\delta} ([D_>(p - k)]^{\nu'\nu} [D_>(k)]^{0\mu} - [D_<(p - k)]^{\nu'\nu} [D_<(k)]^{\mu 0}] \right\}, \end{aligned} \quad (\text{B1})$$

where $p_0 = \omega$. By using the thermal (KMS) relations between the free propagators $D_>, D_<, D_T$ and ρ , this can be further simplified to

$$\begin{aligned} \rho_{\text{adj}}^{++}(\omega) - \rho_{\text{fund}}(\omega) &= \int_{\mathbf{p}, k} \frac{T_F}{3N_c} g^4 N_c (N_c^2 - 1) 2\pi \delta(k_0) [g_{\mu\nu} (p - 2k)_\delta + g_{\nu\delta} (k - 2p)_\mu + g_{\delta\mu} (p + k)_\nu] \\ &\quad \times (p_0 g_{i\delta'} - p_i g_{0\delta'}) ((p_0 - k_0) g_{i\nu'} - (p_i - k_i) g_{0\nu}) \\ &\quad \times (-1) [\rho(p)]^{\delta'\delta} \text{Im} \{ [D_R]^{\nu\nu'}(p - k) \} \text{Im} \{ [D_R]^{\mu 0}(k) \}. \end{aligned} \quad (\text{B2})$$

In our convention, the free propagators in Feynman gauge are given by

$$[\rho(p)]^{\mu\nu} = (-g^{\mu\nu}) (2\pi) \text{sgn}(p_0) \delta(p^2) \quad [D_R(p)]^{\mu\nu} = \frac{-ig^{\mu\nu}}{p^2 + i0^+ \text{sgn}(p_0)}, \quad (\text{B3})$$

and using them to calculate the difference, one arrives at

$$\rho_{\text{adj}}^{++}(\omega) - \rho_{\text{fund}}(\omega) = \int_{\mathbf{p}, \mathbf{k}} \frac{T_F}{3N_c} g^4 N_c (N_c^2 - 1) (2\pi) \delta(k_0) (2\pi) \text{sgn}(\omega) \delta(p^2) \mathcal{P} \left(\frac{2d\omega^3 - 2\omega(\mathbf{p} - \mathbf{k})^2}{k^2(p - k)^2} \right). \quad (\text{B4})$$

In dimensional regularization, $(\mathbf{p} - \mathbf{k})^2$ may be exchanged by ω^2 because $\int_{\mathbf{k}} \frac{1}{k^2}$ vanishes. Then, setting $d = 3$, this integral becomes

$$\rho_{\text{adj}}^{++}(\omega) - \rho_{\text{fund}}(\omega) = \frac{T_F}{3N_c} g^4 N_c (N_c^2 - 1) |\omega|^3 \int_{\mathbf{p}, \mathbf{k}} (2\pi) \delta(p^2) \mathcal{P} \left(\frac{(-4)}{\mathbf{k}^2[\omega^2 - (\mathbf{p} - \mathbf{k})^2]} \right). \quad (\text{B5})$$

The explicit calculation of this integral is equivalent to the one presented in the Supplemental Material of Ref. [35]. The final result is

$$\rho_{\text{adj}}^{++}(\omega) - \rho_{\text{fund}}(\omega) = \frac{T_F}{3N_c} g^4 N_c (N_c^2 - 1) |\omega|^3 \frac{\pi^2}{(2\pi)^3} = \frac{g^4 T_F (N_c^2 - 1) \pi^2}{3(2\pi)^3} |\omega|^3, \quad (\text{B6})$$

as claimed in the main text.

It is noteworthy that the difference between the spectral functions, as given in Eq. (B2) may also be used in conjunction with HTL-resummed propagators to explore the value of the difference (a modification to the gluon 3-vertex is also necessary, according to the HTL effective theory Feynman rules. They can be found in Ref. [70].). However, as discussed in the main text, a full fixed-order calculation at $\mathcal{O}(g^6)$, which is the leading contribution to the difference in the small frequency domain, also requires considering 2-loop diagrams, which we will not pursue here.
